WILEY **morphology**

RESEARCH ARTICLE

Mechanical similarity across ontogeny of digging muscles in an Australian marsupial (*Isoodon fusciventer*)

Meg L. Martin[1] | Natalie M. Warburton[1] | Kenny J. Travouillon[2] | Patricia A. Fleming[1]

[1]School of Veterinary and Life Sciences, Murdoch University, Murdoch, Western Australia, Australia

[2]Department of Terrestrial Zoology, Western Australian Museum, Welshpool, Western Australia, Australia

Correspondence
Meg L Martin, School of Veterinary and Life Sciences, Murdoch University, South Street, Murdoch, WA, 6150, Australia.
Email: m.lane@murdoch.edu.au

Funding information
Murdoch University

Many mammals dig, either during foraging to access subsurface food resources, or in creating burrows for shelter. Digging requires large forces produced by muscles and transmitted to the soil via the skeletal system; thus fossorial mammals tend to have characteristic modifications of the musculoskeletal system that reflect their digging ability. Bandicoots (Marsupialia: Peramelidae) scratch-dig mainly to source food, searching for subterranean food items including invertebrates, seeds, and fungi. They have musculoskeletal features for digging, including shortened, robust forelimb bones, large muscles, and enlarged muscle attachment areas. Here, we compared changes in the ontogenetic development of muscles associated with digging in the Quenda (*Isoodon fusciventer*). We measured muscle mass (m_m), pennation angle, and fiber length (FL) to calculate physiological cross-sectional area (PCSA; a proxy of maximum isometric force) as well as estimate the maximum isometric force (Fmax) for 34 individuals ranging in body size from 124 to 2,390 g. Males grow larger than females in this bandicoot species, however, we found negligible sex differences in mass-specific m_m, PCSA or FL for our sample. Majority of the forelimb muscles PCSA showed a positive allometric relationship with total body mass, while m_m and FL in the majority of forelimb muscles showed isometry. Mechanical similarity was tested, and two thirds of forelimb muscles maximum isometric forces (Fmax) scaled with isometry; therefore the forelimb is primarily mechanical similar throughout ontogeny. PCSA showed a significant difference between scaling slopes between main movers in the power stroke, and main movers of the recovery stroke of scratch-digging. This suggests that some forelimb muscles grow with positive allometry, specially these associated with the power stroke of digging. Intraspecific variation in PCSA is rarely considered in the literature, and thus this is an important study quantifying changes in muscle architectural properties with growth in a mammalian model of scratch-digging.

KEYWORDS

allometry, forelimb muscles, ontogeny, PCSA, Quenda, scratch-digging

1 | INTRODUCTION

Many animals scratch-dig in search of shallow subterranean food, or to construct burrows to shelter themselves and their young from environmental extremes and predators (Shimer, 1903). Fossorial and semi-fossorial mammals are categorized by their principal mode of excavating soil (Table 1). Of these, scratch-digging, in which soil loosened by clawed forelimbs using a running motion (using an alternating limb cycle of retraction-power stroke, and protraction-recovery stroke) in a parasagittal plane, is the most common mode of digging

used in mammals. Scratch-digging mammals are characterized by morphological modifications of their forelimbs that allow them to produce large out-forces that act against the resistance of the soil (Hildebrand, 1985; Rose, Sandefur, Huskey, Demler, & Butcher, 2013).

If limb segments are modeled as simple lever systems, the mechanical advantage is dependent on the ratio of in-lever length to out-lever length and the magnitude of the in-force (Hildebrand, 1985). As a result, the limb bones in scratch-digging mammals are short and robust to reduce the out-lever length, main mover muscles during the power stroke of scratch-digging are enlarged to increase the

TABLE 1 Summary of the four modes of digging in mammals

	Description	Actions	Examples	References
Scratch-digging	Soil loosened by clawed forelimbs using a running motion in a parasagittal plane.	• Humeral retraction • Elbow extension • Carpal flexion • Digit flexion	e.g., bandicoots and bilbies (Peramelemorphia), wombats (Vombatidae), potoroos (Potoroidae), badgers (Mustelidae), armadillos (Dasypodidae), groundhogs (Sciuridae)	(Hildebrand, 1985; Moore, Budny, Russell, & Butcher, 2013; Olson, Womble, Thomas, Glenn, & Butcher, 2015; Vassallo, 1998; Warburton, Grégoire, Jacques, & Flandrin, 2013)
Chisel-tooth digging	Gnaw soil with incisors to excavate their burrows.	• Incisors increased procumbency • Jaw adductors • Jaw stabilisation	e.g., rodents (Octodontids, Ctenomyids), mole-rats (Bathyergidae)	(Hildebrand, 1985; Hopkins & Davis, 2009; McIntosh & Cox, 2016a, 2016b)
Humeral-rotation	Sprawling, abducted forelimb posture, and involves a rotation of the humerus while the forelimb extends to sweep the soil behind.	• Humeral rotation • Elbow extension • Manus held between supination and pronation	e.g., moles (Talpidae), echidnas (Tachyglossidae)	(Barnosky, 1981; Hopkins & Davis, 2009)
Head-lift digging	Snout and forelimbs to wedge open the tunnel where they permanently reside.	• Head elevation • Push firmly down with the forelimbs	e.g., Golden moles (Chrysochloridae), mole voles (Cricetidae), mole-rats (Bathyergidae)	(Gasc, Jouffroy, Renous, & Blottnitz, 1986; Hildebrand, 1985; Stein, 2000)

Fossorial animals (those that are morphologically or physiologically adapted for digging, yet are mostly active above ground) are categorized by their principal mode of excavating soil, of which, scratch-digging is the most common used mode of digging in mammals. Subterranean animals (species that are highly specialized for living almost wholly underground) show further specialisations for scratch-digging and/or resort to other digging modes (Lessa & Thaeler 1989).

magnitude of the in-force, and the attachment sites of these muscles are moved further away from the joint (center of rotation) to increase the in-lever length (Hildebrand, 1985; Lagaria & Youlatos, 2006; Rose, Moore, Russell, & Butcher, 2014; Shimer, 1903; Warburton, Grégoire, et al., 2013). Forelimb muscles involved in humeral stabilization, humeral retraction, and elbow extension are capable of producing large out-forces during the power stroke (Hildebrand, 1985; Lagaria & Youlatos, 2006). For example, Quenda (*Isoodon fusciventer*) have large and powerful muscles associated with humeral retraction, elbow extension, and carpal and digital flexion (Warburton, Grégoire, et al., 2013). The bones of the forelimb have enlarged muscle attachment areas, relatively long in-levers, such as an elongate olecranon process for the insertion of the elbow extensors, and the humerus, radius, and ulna are short and robust (Warburton, Grégoire, et al., 2013). These specializations provide improved mechanical advantage for scratch-digging.

Muscle ultrastructure reflects contractile velocity and force production, and is therefore also likely to demonstrate specializations for digging. Fiber length (FL) represents the number of sarcomeres in a series (Michilsens, Vereecke, D'Août, & Aerts, 2009), and consequently longer fibers have faster shortening velocity (Azizi, Brainerd, & Roberts, 2008; Kikuchi, 2010; Lieber & Fridén, 2000). In digging animals such as badgers (*Taxidea taxus*; Moore et al., 2013), groundhogs (*Marmota monax*; Rupert, Rose, Organ, & Butcher, 2015), and armadillos (*Dasypus novemcinctus*; Olson et al., 2015), longer fibers in muscles such as the latissimus dorsi, pectoralis, triceps brachii, and teres major provide rapid fiber contraction during the power stoke of scratch-digging. The force a muscle produces is influenced by the arrangement of the muscle fibers (number of sarcomeres in parallel; Lieber & Ward, 2011; Rupert et al., 2015). Physiological cross-sectional area (PCSA) is calculated from muscle mass (m_m) and muscle architecture data; fiber length (FL) and pennation angle (the angle between the line of action of the muscle and the fibers), and is considered a better representation of muscle force production than muscle mass alone (Moore et al.,

2013). As PCSA is a representation of maximum isometric force production for individual muscles, the PCSA values of muscles in a limb can be used to interpret biological functions in correlation with skeletal morphology (Myatt et al., 2012; Thorpe, Crompton, GÜnther, Ker, & McNeill, 1999). Scratch-digging mammals have relatively large PCSA values for muscles used as main movers in the power stroke, such as the triceps brachii long head, which reflect a greater number of fibers per unit volume of muscles; this allows them to produce a greater force for scratch-digging (Moore et al., 2013; Olson et al., 2015; Rose et al., 2013; Rupert et al., 2015).

Bandicoots (Peramelidae) are typically omnivorous and use scratch-digging to search for subterranean food sources. When moving, bandicoots use an asymmetrical half-bound gait similar to many other marsupial taxa (Bennett & Garden, 2004; Hildebrand, 1977). This mode of locomotion, being powered primarily by the hindlimbs, allows bandicoots to retain specialized forelimbs for digging (Bennett & Garden, 2004; Gordon & Hulbert, 1989). Quenda are commonly found throughout south-west Western Australia. The Quenda produces an average of 45 foraging pits per day (Valentine, Anderson, Hardy, & Fleming, 2013) as they search for subterranean food sources. Each dig is conical in shape, measuring 35–135 mm in depth, and an average-sized (1.4 kg) Quenda is estimated to move 2.8 tons of soil per year. As the presence of digging mammals is known to improve soil quality, the presence of bandicoots has the potential to greatly impact their local ecological community, and these animals are therefore considered ecosystem engineers (Fleming et al., 2014; Valentine et al., 2013).

Scaling muscle architectural properties (such as individual m_m, FL, or PCSA) against total body mass are commonly used to investigate locomotor adaptations, or used to describe intraspecific biomechanical constraints across a range of body sizes (Allen et al., 2014; Allen, Elsey, Jones, Wright, & Hutchinson, 2010; Lamas, Main, & Hutchinson, 2014; Picasso, 2015) or among species (Bertram & Biewener, 1990; Cuff et al., 2016). A scaling muscle architecture study has not been used to

investigate Australian digging marsupials. We compared ontogenetic changes in the forelimb muscles in *Isoodon fusciventer*, testing the prediction that muscles that are main movers during the power stroke of scratch-digging would show steeper allometric growth compared with the muscles that are more associated with the recovery stroke of scratch-digging, reflecting modifications associated with large out-force production in these scratch-digging mammals.

2 | MATERIALS AND METHODS

2.1 | Specimens

Quenda were recently raised to species level on the basis of cranio-dental morphology and molecular data compared to the other subspecies in *Isoodon obesulus* (Travouillon & Phillips, 2018) (Figure 1). Their ability to adapt to an urban environment has come with risks, as Quenda are susceptible to dog attacks and collisions with cars; these were the primary reasons of death for the specimens collected. Bandicoot cadaver specimens ($n = 34$) were collected from Kanyana Wildlife Rehabilitation Centre (Lesmurdie, Western Australia), or opportunistically collected throughout the Perth metropolitan area (Regulation 17 licence SF010344). Details of specimens are presented in Supporting Information Table S1. Quenda are sexually dimorphic in body size (body mass m_b range; males: 500–1,850 g, females: 400–1,200 g) (Warburton & Travouillon, 2016), and therefore, we were mindful of potential sex differences in our analyses.

Specimens were stored frozen (−18 °C), and defrosted for 48 hr in refrigerated conditions (4 °C) prior to dissection. Total body mass (m_b) was recorded (± 0.1 g; Phoenix Scales Ltd., West Bromwich, UK) and then specimens were skinned, eviscerated, and embalmed in a solution of 10% formalin and 4% glycerol for 7 days before transfer to 70% ethanol for storage until muscle dissection. Specimens were preserved in formalin for the study due to the nature of specimen collection; road kill specimens have substantial damage, therefore, fixing the specimens allowed the forelimbs to be used in the study. Entire bodies were fixed with the forelimbs and hindlimbs fixed in the resting anatomical position (as close to a 90° angle that could be achieved) to minimize the effect of changing (shortening or lengthening) the lengths of the muscles and therefore muscle architecture. All muscle architectural measurements were corrected using correction factors published for fixed muscle tissue (Kikuchi & Kuraoka, 2014).

2.2 | Muscle dissection

Muscle dissections were performed using standard dissection techniques and followed muscle descriptions (names, origins, and insertions) and methods by Warburton, Grégoire, et al. (2013). Right forelimbs were dissected unless damage had occurred, in which case the left forelimb was dissected. Individual muscles were isolated and removed, and muscle mass recorded (m_m, ±0.001 g; Mettler Toledo BB240 Precision Balance, Toronto Surplus & Scientific Inc., Richmond Hill Canada).

Photographs of isolated muscle bellies (Olympus Stylus Tough TG-3 Digital Camera, Olympus Australia, Pty Ltd., Notting Hill, Australia) were used to determine pennation angle. Pennation angles were measured on photographs using the "angle" tool in ImageJ

(Version 1.49) (Abramoff, Magalhaes & Ram 2004) at 10 randomized locations throughout the muscle belly. Muscles were placed in 30% nitric acid for 24 hr to loosen the connections between fibers, then washed in water and soaked in 30% glycerol for 1–2 hr. This process allowed individual muscle fibers to be teased apart using blunt forceps. Superficial fibers were avoided as they tended to be longer, therefore 10 deeper fibers were randomly selected for measurement of FL. PCSA was calculated:

$$\text{PCSA (cm}^2) = \frac{m_m \text{ (g) x pennation angle (cos } \theta)}{\text{muscle density (g/cm}^3) \text{ x FL (cm)}}$$

where an estimate of vertebrate muscle density (1.06 g/cm^3; Mendez & Keys, 1960) was used as the muscle density constant. To permit for the most accurate estimate of the maximum isometric force (Fmax; Moore et al., 2013; Williams, Wilson, Rhodes, Andrews, & Payne, 2008), we multiplied the PCSA (cm^2) by a maximum isometric stress of 30 N/cm^{-2} (Medler, 2002).

2.3 | Statistical analysis

Twenty-nine muscles were classified for statistical analyses into nine functional groups (Table 2). Muscles involved in scapula stabilization (SS), humeral retraction (HR), elbow extension (EE), carpal/digital flexion (CF), and pronation (PRO) where considered to be active during the power stroke of scratch-digging, whereas the functional groups involved in humeral protraction (HP), elbow flexion (EF), carpal/digital extension (CE), and supination (SUP) were classified as active during the recovery stroke (Figure 1). While we acknowledge that many muscles will have more than one action, this simplified view was taken to allow comparison between muscles classified as main movers in the power stroke vs. recovery stroke during scratch-digging.

The four muscle architectural properties (m_m, FL, PCSA, Fmax) were log$_{10}$-transformed and analyzed against log$_{10}$-total body mass (m_b). We tested for potential sex differences in the slopes of these relationships by Analysis of Covariance (ANCOVA), with sex (males: 0, females: 1) as a fixed factor and m_b as the covariate. To calculate the slopes of the relationships between the muscle architectural properties and m_b, we used reduced major axis (RMA; Model II) regression in PAST version 3.16 (Paleontological Statistics; http://folk.uio.no/ohammer/past/; Hammer, Harper, & Ryan, 2001). All scaling regressions were assessed using Shapiro–Wilk tests (Quinn & Keough, 2002). Correlation coefficients (Pearson's Moment correlation) and upper and lower bounds of the 95% confidence intervals were calculated to evaluate the data spread around each regression. To consider different properties as geometrically similar, and thus infer the scaling pattern, the measures must be scaled following the rules of isometry. Muscle properties were considered isometric for masses (m_m) and force (Fmax) if they scale with $m_b^{1.0}$, areas (i.e., PCSA) if they scale to $m_b^{0.67}$, and lengths (i.e., FL) if they scale to $m_b^{0.33}$. The slopes (β) of the individual muscles were tested against the null hypotheses of $\beta = 1$ (m_m), $\beta = 0.67$ (PCSA), or $\beta = 0.33$ (FL) by calculating the t ratio = (β-1.0, 0.67, or 0.33)/standard error of the slope. To test if the muscles are mechanically similar throughout ontogeny, the slope of Fmax with total body mass was tested against the null hypothesis of the slope of 1.0 (Rose, 2014). We estimated the false discovery rate (FDR) to determine

TABLE 2 Average values of muscle mass (m_m), fiber length (FL), pennation angle, physiological cross-sectional area (PCSA) and isometric force (Fmax) of each individual muscle calculated from 29 Quenda (*Isoodon fusciventer*). Muscles are sorted by functional groups and then from proximal to distal

	Abb.	Funct	Muscle mass	Fiber length	Pennation	PCSA	Fmax
Trapezius	Trap	SS	3.94 ± 2.49	1.81 ± 0.83	28 ± 7	1.82 ± 1.10	54.57 ± 32.48
Omotransversarius	OmT	SS	1.05 ± 0.68	1.69 ± 0.60	11 ± 9	0.57 ± 0.33	17.06 ± 10.14
Rhomboideus	Rho	SS	2.11 ± 1.71	1.46 ± 0.54	26 ± 11	1.13 ± 0.65	33.98 ± 19.21
Serratus ventralis	SeV	SS	5.83 ± 4.36	1.84 ± 0.68	12 ± 10	2.90 ± 2.29	87.08 ± 67.62
Latissimus dorsi	LtD	HR	3.19 ± 2.17	1.88 ± 0.94	22 ± 8	1.53 ± 0.87	45.78 ± 25.89
Pectoralis	Pec	HR	9.85 ± 6.63	1.85 ± 0.70	27 ± 10	4.18 ± 2.29	125.33 ± 67.93
Deltoideus	Delt	HR	0.50 ± 0.33	1.03 ± 0.30	29 ± 9	0.38 ± 0.22	11.44 ± 6.36
Infraspinatus	Inf	HR	1.45 ± 1.03	0.94 ± 0.22	25 ± 5	1.24 ± 0.72	37.15 ± 21.41
Teres major	TMj	HR	1.14 ± 0.78	1.07 ± 0.51	21 ± 7	0.91 ± 0.50	27.21 ± 14.77
Subscapularis	Sub	HR	1.63 ± 1.16	0.89 ± 0.22	24 ± 12	1.50 ± 0.90	44.88 ± 26.63
Triceps brachii	TrB	EE	4.99 ± 3.41	1.36 ± 0.44	23 ± 7	3.12 ± 1.88	93.54 ± 55.74
Anconeus	Anc	EE	0.19 ± 0.14	0.85 ± 0.28	NA	0.20 ± 0.13	6.13 ± 3.83
Tensor fascia antebrachii	TFA	EE	0.81 ± 0.70	1.53 ± 0.72	NA	0.49 ± 0.35	14.57 ± 10.49
Flexor carpi radialis	FCR	CDF	0.26 ± 0.20	0.78 ± 0.19	19 ± 7	0.29 ± 0.18	8.56 ± 5.22
Flexor carpi ulnaris	FCU	CDF	0.25 ± 0.20	0.68 ± 0.19	35 ± 7	0.27 ± 0.19	8.09 ± 5.70
Palmaris longus	PaL	CDF	0.20 ± 0.16	0.82 ± 0.20	20 ± 6	0.20 ± 0.14	5.98 ± 4.08
Flexor dig. Superficialis	FDS	CDF	0.21 ± 0.14	0.95 ± 0.23	20 ± 11	0.18 ± 0.12	5.49 ± 3.53
Flexor dig. Profundus	FDP	CDF	1.76 ± 1.26	0.98 ± 0.24	25 ± 7	1.41 ± 0.83	42.36 ± 24.51
Pronator teres	PrT	PRO	0.20 ± 0.13	0.74 ± 0.13	24 ± 6	0.22 ± 0.13	6.52 ± 3.95
Pronator quadratus	PrQ	PRO	0.05 ± 0.03	0.40 ± 0.09	NA	0.11 ± 0.07	3.22 ± 2.21
Supraspinatus	Sup	HP	1.80 ± 1.22	1.07 ± 0.27	25 ± 5	1.41 ± 0.82	42.37 ± 24.28
Biceps brachii	BiB	HP/EF	0.56 ± 0.41	1.06 ± 0.30	16 ± 6	0.47 ± 0.28	13.96 ± 8.32
Brachialis	Bra	EF	0.68 ± 0.45	1.13 ± 0034	22 ± 7	0.51 ± 0.28	15.33 ± 8.32
Extensor carpi radialis	ECR	CDE	0.55 ± 0.34	1.05 ± 0.32	22 ± 6	0.46 ± 0.27	13.95 ± 8.00
Extensor dig. Communis	EDC	CDE	0.38 ± 0.25	1.01 ± 0.18	19 ± 8	0.33 ± 0.20	10.02 ± 6.03
Extensor dig. Lateralis	EDL	CDE	0.09 ± 0.07	0.86 ± 0.27	10 ± 10	0.10 ± 0.08	3.11 ± 2.45
Extensor carpi ulnaris	ECU	CDE	0.16 ± 0.10	0.72 ± 0.19	16 ± 8	0.22 ± 0.16	6.63 ± 4.84
Abductor digiti I longus	AbdL	CDE	0.10 ± 0.07	0.68 ± 0.22	NA	0.15 ± 0.11	4.40 ± 3.17
Supinator	Spr	SUPI	0.10 ± 0.07	0.57 ± 0.20	NA	0.18 ± 0.19	5.35 ± 5.71

Standard deviations displayed and the abbreviations of all the muscles that are used throughout the study. NA in pennation angle represents muscles that display parallel fibers and no pennation.

Abbreviations: SS = Scapula stabilization; HR = humeral retraction; EE = elbow extension; CDF = carpal/digital flexion; PRO = pronators; HP = humeral protraction; EF = elbow flexion; CDE = carpal/digital extension; SUPI = supinators.
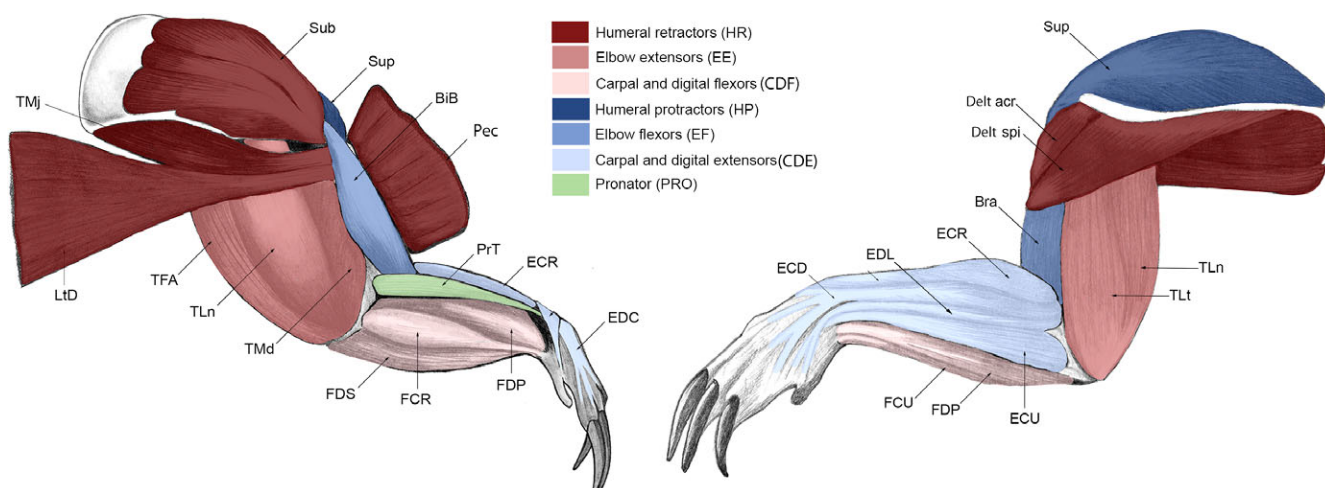

FIGURE 1 Musculature of the forelimb muscles of the Quenda (*Isoodon fusciventer*). Each colour represents a different functional muscle group. (a) Superficial medial view altered from (Warburton, Grégoire, et al., 2013) and (b) superficial lateral view. Abbreviations: BiB = Biceps brachii; bra = Brachialis; Del acr & Del spi combined for Delt = Deltoideus; ECR = Extensor carpi radialis; ECU = Extensor carpi ulnaris; EDC = Extensor digitorum communis; EDL = Extensor digitorum lateralis; FCR = Flexor carpi radialis; FCU = Flexor carpi ulnaris; FDP = Flexor digitorum profundus; FDS = Flexor digitorum superficialis; Inf: Infraspinatus; LtD = Latissimus dorsi; Pec = Pectoralis; PrT = Pronator teres; sub = Subscapularis; sup = Supraspinatus; TFA = Tensor fascia antebrachii; TMj = Teres major; TLn & TMd combined for TrB = Triceps brachii

which slopes were significantly different from the geometric slope (Benjamini & Hochberg, 1995) to control for Type 1 errors. Mann–Whitney U test was used to compare the slopes (β) of power stroke and recovery stroke muscles.

Values are presented as means ±1SD throughout.

3 | RESULTS

3.1 | Is there a significant sex difference in forelimb development?

In our sample, male Quenda specimens (1,041 ± 667 g, range 124–2,390 g, n = 21) were not significantly larger than females (810 ± 356 g, range 208–1,320 g, n = 13; t_{32} = −1.15 p = 0.259). The mean total forelimb mass for our sample of Quenda was 43.2 ± 29.6 g (male) and 31.2 ± 15.0 g (female), which accounts for 4.0 ± 0.5% (male) and 3.8 ± 0.3% (female) of the total body mass. There was no significant sex difference in total forelimb mass (t_{32} = −1.65 p = 0.109).

Forelimb muscle mass was distributed in a proximal-distal gradient, with larger muscles positioned closer to the shoulder joint (Table 2). Nearly half of the forelimb m_m was attributed to humeral retraction (HR, 40.4 ± 3.36%), while scapula stabilization (SS, 29.2 ± 3.46%), elbow extension (EE, 13.6 ± 1.25%) and carpal/digital flexion (CDF, 6.03 ± 0.58%) contributed the next three largest proportions of the forelimb mass; the other five functional group each contributed less than 5% of the forelimb mass (Figure 2). Males and females had a slightly different distribution of muscles throughout the limb (Figure 2). Compared with females, males had relatively heavier forearm muscles: elbow flexors (EF) and extensors (EE), carpal/digital flexors (CDF), humeral protractors (HP), and the pronators (PRO).

There were negligible sex differences in forelimb muscle architectural properties (analysis of covariance testing for sex differences in the scaling relationships with m_b for each of the three muscle architecture measures [m_m, FL, PCSA] of the 29 individual forelimb muscles; Figure 3). Only one relationship (of the total 87 total measurements analysed) showed a significant sex effect (muscle mass of the tensor fascia antebrachii [TFA]; p = 0.027), which had a significantly steeper slope (positive allometry) in males than females. Sex was included as a factor in the analyses of slopes to account for any potential sex differences, although the sex effect will not be described in any further detail.

3.2 | Do digging power stroke muscles show greater positive allometry compared with recovery stroke muscles?

Forelimb muscle masses (m_m) were strongly correlated with m_b; 26 of the 29 muscles had correlation coefficient values r > 0.90 (Table 3). The slopes for all of the muscles except flexor carpi radialis (FCR) were greater than 1, and only half the muscles had 95% confidence intervals that included the line of geometric similarity (β = 1; Figure 4). The slopes for six muscles (all classed as main movers in the power stroke of scratch-digging) were statistically different from β = 1.

Compared with the muscle mass values, measures of FL, generally showed weaker correlations with m_b (most muscles had r < 0.60; Table 3). The majority of forelimb muscles had slopes steeper than β = 0.33 (the value reflecting geometric similarity for this linear measure) indicating they may be developing with positive allometry. Only five of these muscles were statistically significantly different from a slope of 0.33 (Figure 4); four muscles (of 20) were associated with the power stroke, and one (of nine) in the recovery stroke of scratch-digging.

Values of PCSA for all muscles were significantly correlated with m_b, with the majority of the muscles (25/29) having correlation
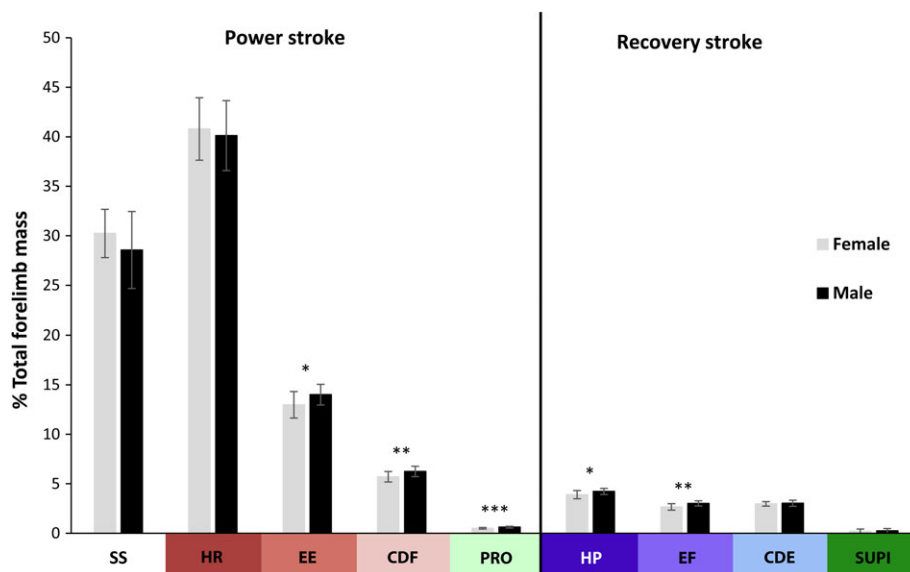

FIGURE 2 Average (±1SD) proportions of total forelimb muscle mass represented by each of the nine functional groups. Functional groups are separated into muscles associated with either the power stroke or recovery stroke in scratch-digging and ordered from proximal to distal muscle. There were sex differences in distribution of muscle mass (t test), and therefore the data are shown organized by sex where * p < .05, ** p < .01, *** p < .001. Functional group abbreviations are defined in Table 2. Black bars: Male, gray bars: Female. Functional groups are ordered proximal to distal
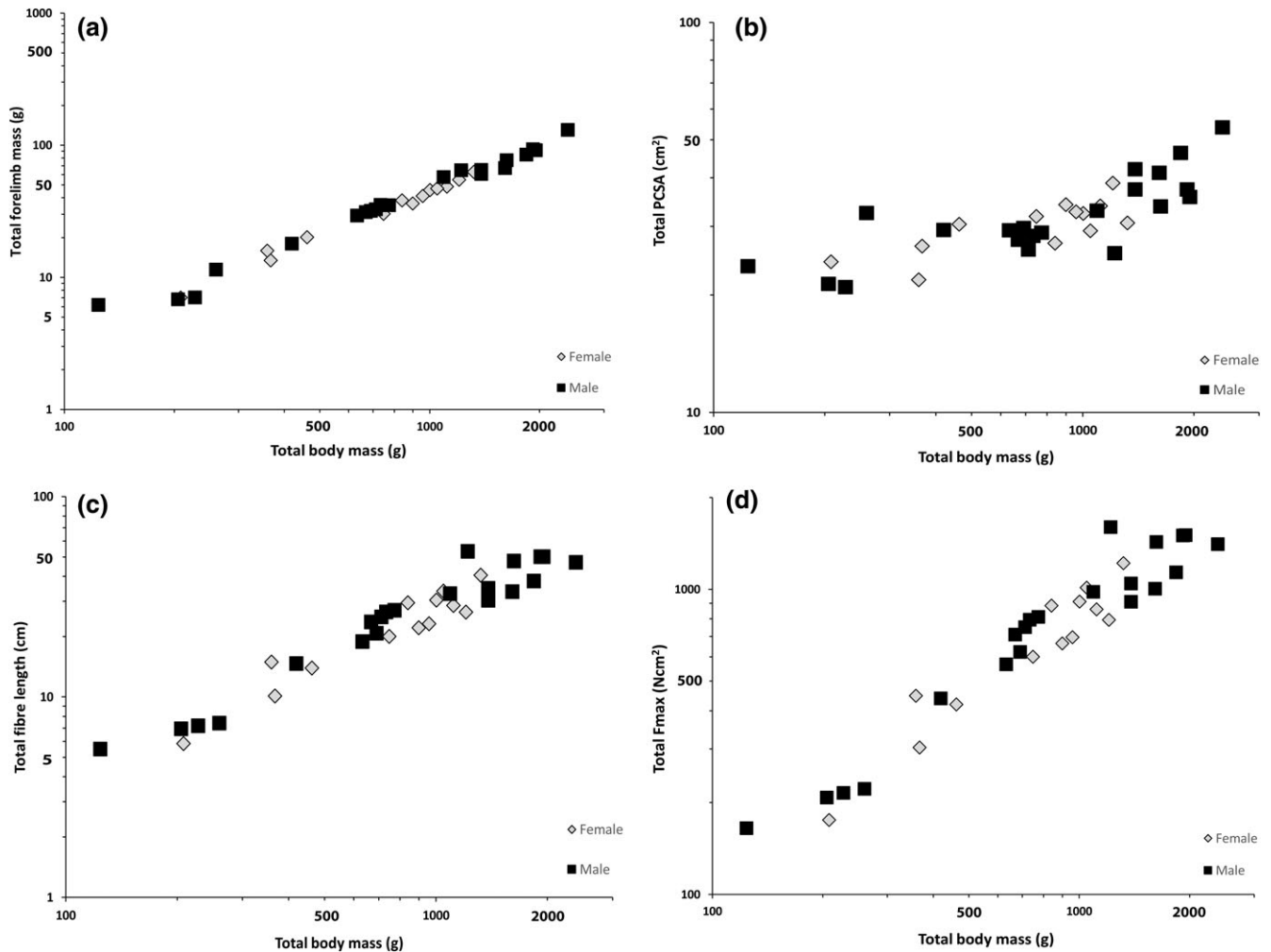
FIGURE 3 Relationship between total body mass muscles architectural properties plotted on a log scale. Total muscle architectural properties are calculated by summing the muscle property values for all the individual muscles. (a) Total forelimb mass (g), (b) total fiber length (cm), (c) total PCSA (cm^{-2}), and (d) total isometric force (Fmax; Ncm^{-2}). All the four muscle architectural properties showed a strong positive relationship with total body mass. Black squares: Males, Gray diamonds: Females

coefficient values >0.8 (Table 3). Of the 29 muscles, 18 had slopes that were significantly different from 0.67 (geometric similarity for this area measure) indicating that they increased with strong positive allometry. Both muscles that are main movers in the power stroke, and muscles associated with the recovery stroke of digging, showed positive allometry.

The slope of isometric force (Fmax) was significantly correlated with m_b and about a third of the muscles (11/29) had significantly different slopes from 1.0 (mechanical similarity). Ten of the muscles statistically different from mechanical similarity were active during the power stroke, while brachialis (BRA) was the only muscle active during the recovery stroke.

The Quenda forelimb had some muscles that had relatively greater PCSA and long FL that indicated the capacity for greater power (Figure 5). The pectoralis (Pec), triceps brachii (TrB) and serratus ventralis (SeV) occupied the high power quadrant, while no muscles were in the force-specialized quadrant. While the larger muscles acting across the shoulder joint are expected to be more powerful, we saw that the largest elbow extensor, triceps brachii (TrB), was more powerful that the shoulder stabilizers and humeral retractors such as the latissimus dorsi (LtD) and rhomboideus (Rho).

The scaling slopes of the muscles associated with the power stroke of digging, and muscles associated with the recovery stroke of digging were not significantly different for the muscles masses ($Z_{n = 20,9} = 0.660$, $p = 0.509$) and FL ($Z_{n = 20,9} = 0.825$, $p = 0.409$), however, the scaling slopes of PCSA showed a significant difference between the muscles associated with the two phases of scratch-digging ($Z_{n = 20,9} = -2.71$, $p = 0.007$) with shallower slopes for muscles active during the power stroke of scratch-digging.

4 | DISCUSSION

We have presented the first study on ontogenetic scaling of the forelimb muscle architectural properties in a digging mammal, using 34 Quenda across a large range of body masses. In our study, the majority of muscle PCSA values scaled with positive allometry, while m_m and FL primarily showed isometry. During growth, there appears to be strong investment in muscles associated with the power stroke of scratch-digging, and these muscles account for 90% of the total forelimb muscle mass (range between 88 and 91%).

TABLE 3 Regression analysis results for the log-transformed muscle architecture properties vs. log-transformed total body mass of the Quenda (*Isoodon fusciventer*) forelimb muscles. The lower and upper 95% confidence intervals demonstrate the scaling relationship–gray-shaded cells highlight where the confidence intervals range did not included the line representing isometry

Muscle	Abbv.	Funct.	m_m v m_b r	Slope (β)	Std. err. β	Range (95% CI)	p (β = 1)	FL v m_b r	Slope (β)	Std. err. β	Range (95% CI)	p (β = 0.33)	$PCSA$ v m_b r	Slope (β)	Std. err. β	Range (95% CI)	p (β = 0.67)	F_{max} v m_B p (β = 1)
Trapezius	Trap	SS	0.979	1.059	0.012	0.968–1.140	0.348	0.602	0.548	0.050	0.377–0.679	0.015*	0.796	0.877	0.074	0.662–1.060	0.767	**0.002**
Omotransversarius	OmT	SS	0.961	1.117	0.025	1.034–1.225	0.180	0.589	0.501	0.043	0.353–0.630	0.018*	0.809	0.964	0.084	0.750–1.129	0.272	0.037*
Rhomboideus	Rho	SS	0.955	1.099	0.028	1.000–1.205	0.389	0.592	0.419	0.030	0.261–0.551	0.020*	0.914	0.903	0.035	0.793–1.007	0.022	**0.012**
Serratus ventralis	SeV	SS	0.962	1.256	0.031	1.119–1.360	**0.002**	0.648	0.504	0.039	0.348–0.622	**0.002**	0.833	1.082	0.094	0.844–1.261	0.034*	0.366
Latissimus dorsi	LtD	HR	0.986	1.135	0.01	1.054–1.197	**0.001**	0.533	0.646	0.079	0.441–0.828	0.024*	0.840	0.962	0.072	0.738–1.140	0.145	0.043*
Pectoralis	Pec	HR	0.965	1.135	0.023	1.016–1.262	0.078	0.696	0.492	0.033	0.362–0.597	**0.001**	0.865	0.867	0.050	0.709–1.005	0.315	**0.003**
Deltoideus	Delt	HR	0.964	1.029	0.02	0.912–1.121	0.865	0.624	0.402	0.026	0.259–0.511	0.069	0.876	0.864	0.046	0.734–0.967	0.254	**0.002**
Infraspinatus	Inf	HR	0.985	1.165	0.011	1.076–1.259	**p < 0.001**	0.567	0.323	0.019	0.192–0.410	0.505	0.954	1.018	0.024	0.915–1.109	**p < 0.001**	0.605
Teres major	TMj	HR	0.975	1.091	0.015	0.997–1.191	0.139	0.630	0.461	0.034	0.246–0.640	0.044*	0.895	0.880	0.040	0.780–0.967	0.098	**0.004**
Subscapularis	Sub	HR	0.975	1.114	0.016	0.994–1.224	0.055	0.455	0.337	0.024	0.200–0.425	0.869	0.935	1.024	0.035	0.920–1.145	**p < 0.001**	0.522
Triceps brachii	TrB	EE	0.983	1.078	0.01	0.984–1.176	0.094	0.484	0.429	0.037	0.275–0.522	0.095	0.894	0.956	0.048	0.790–1.090	**0.017**	0.065
Anconeus	Anc	EE	0.884	1.113	0.071	0.952–1.248	0.858	0.547	0.426	0.033	0.268–0.527	0.345	0.800	0.935	0.083	0.760–1.056	0.447	**0.016**
Tensor fascia antebrachii	TFA	EE	*0.972	1.224	0.022	1.097–1.345	**0.001**	0.589	0.556	0.053	0.379–0.701	**0.009**	0.869	0.993	0.064	0.801–1.152	**0.033**	0.119
Flexor carpi radialis	FCR	CDF	0.819	0.991	0.085	0.827–1.132	0.068	0.613	0.302	0.015	0.206–0.372	0.930	0.737	0.867	0.090	0.683–1.006	0.773	**0.001**
Flexor carpi ulnaris	FCU	CDF	0.967	1.195	0.025	1.049–1.333	**0.009**	0.543	0.354	0.023	0.230–0.439	0.757	0.911	1.082	0.052	0.929–1.225	**0.001**	0.859
Palmaris longus	PaL	CDF	0.966	1.156	0.024	1.027–1.295	0.036*	0.632	0.320	0.016	0.217–0.391	0.652	0.933	0.977	0.032	0.846–1.108	**0.001**	0.165
Flexor dig. Superficialis	FDS	CDF	0.941	1.099	0.036	0.934–1.238	0.602	0.647	0.325	0.016	0.250–0.386	0.180	0.881	0.912	0.049	0.727–1.077	0.087	**0.014**
Flexor dig. Profundus	FDP	CDF	0.98	1.148	0.014	1.039–1.254	**0.003**	0.745	0.371	0.016	0.261–0.455	0.017*	0.939	0.887	0.025	0.766–0.982	**0.006**	**0.003**
Pronator teres	PrT	PRO	0.957	1.066	0.025	0.943–1.200	0.714	0.641	0.237	0.009	0.173–0.287	0.187	0.873	1.057	0.070	0.789–1.258	**0.010**	0.068
Pronator quadratus	PrQ	PRO	0.833	1.001	0.081	0.749–1.172	0.095	0.534	0.347	0.023	0.242–0.441	**0.001**	0.737	0.879	0.093	0.593–1.068	0.836	**0.003**
Supraspinatus	Sup	HP	0.985	1.103	0.01	1.020–1.192	0.016*	0.422	0.353	0.027	0.223–0.440	0.662	0.923	1.022	0.041	0.873–1.145	**0.001**	0.421
Biceps brachii	BiB	HP/EF	0.974	1.119	0.017	1.028–1.213	0.053	0.455	0.365	0.028	0.198–0.477	0.390	0.913	1.025	0.046	0.889–1.135	**0.001**	0.387
Brachialis	Bra	EF	0.975	1.02	0.014	0.919–1.128	0.887	0.542	0.393	0.029	0.270–0.480	0.183	0.921	0.881	0.031	0.782–0.975	**0.028**	**0.004**
Extensor carpi radialis	ECR	CDE	0.983	1.055	0.01	0.966–1.146	0.286	0.218	0.392	0.039	0.276–0.432	0.456	0.911	1.045	0.049	0.838–1.216	**0.001**	0.534
Extensor dig. Communis	EDC	CDE	0.96	1.053	0.023	0.922–1.194	0.827	0.217	0.237	0.014	0.147–0.574	0.051	0.942	1.029	0.031	0.881–1.173	**p < 0.001**	0.608
Extensor dig. Lateralis	EDL	CDE	0.925	1.21	0.056	1.050–1.347	0.143	0.172	0.430	0.047	0.250–0.574	0.190	0.826	1.247	0.130	1.013–1.432	**0.008**	0.814
Extensor carpi ulnaris	ECU	CDE	0.978	1.12	0.015	1.025–1.212	0.030*	0.173	0.389	0.039	0.213–0.534	**0.001**	0.941	1.216	0.044	1.083–1.344	**p < 0.001**	0.056
Abductor digiti longus	AbdL	CDE	0.959	1.124	0.027	0.984–1.283	0.184	0.336	0.425	0.042	0.253–0.564	0.397	0.887	1.053	0.062	0.860–1.219	**0.005**	0.462
Supinator	Spr	SUPI	0.959	1.071	0.024	0.947–1.173	0.614	0.235	0.345	0.050	0.282–0.426	0.136	0.873	1.057	0.070	0.789–1.258	**0.010**	0.397

Abbreviations: SS = Scapula stabilisation; HR = Humeral retraction; EE = Elbow extension; CDF = Carpal/digital flexion; EF = Elbow flexion; CDE = Carpal/digital extension; HP = Humeral protraction; PRO = Pronators; SUPI = Supinators.

Results with significant *p*-values are highlighted in bold which indicated that the muscle scaling relationship is significantly different to isometry. *p*-values with a * are *p*-values that are no longer significant using the FDR. Muscles are separated into groups associated with the power stroke or the recovery stroke of scratch-digging, and within these two groups muscles are ordered as proximally to distally placed muscles.
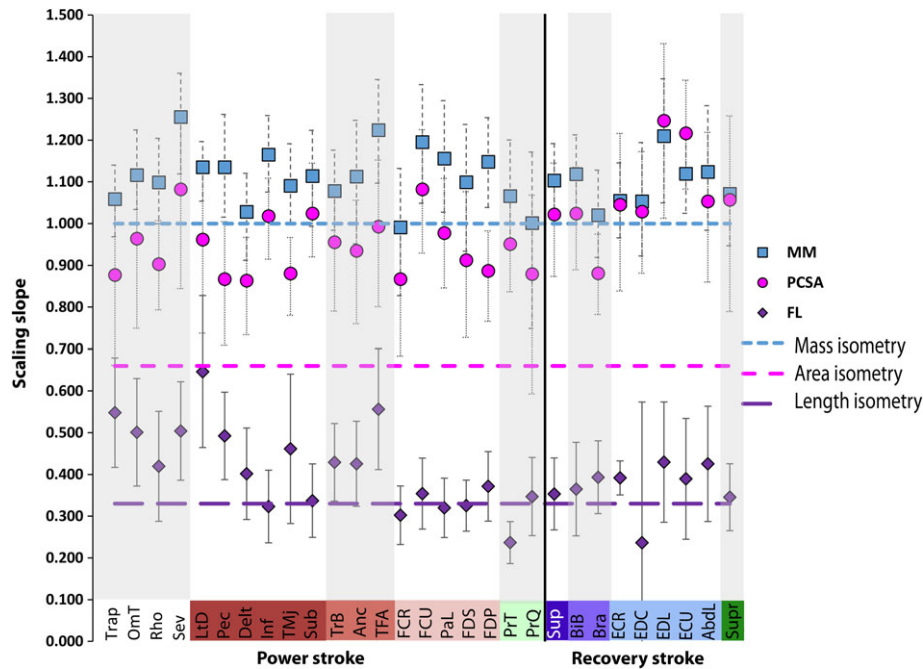
FIGURE 4 The 95% confidence intervals for scaling slopes of forelimb log architectural properties on log total body mass in Quenda (*Isoodon fusciventer*). Blue squares indicate the regression slopes for muscle mass (m_m); pink circles indicate regression slopes for PCSA; and purple diamonds indicate regression slopes for fiber length (FL). The error bars show the upper and lower 95% confidence intervals, and dashed lines indicate the relevant value for isometry. Muscles are separated into muscles associated with the power stroke or recovery stroke of scratch-digging as well as ordered as most proximally placed muscles to most distally placed muscles. Majority of the muscle masses and PCSA slopes are scaling above isometry, while the FL are scaling closer to isometry

FIGURE 5 Functional space plot (fiber length vs. PCSA) for muscles in the forelimb of Quenda, *Isoodon fusciventer*. Normalized PCSA is normalized to body mass[(0.67)] and normalized FL is normalized to body mass[(0.33)]. Data points are means with no error bars shown. Quadrant definitions were based off the literature (Allen et al., 2010; Böhmer, Fabre, Herbin, Peigné, & Herrel, 2018; Channon, Günther, Crompton, & Vereecke, 2009; Dick & Clemente, 2016). High force is defined as high PCSA and shorter fiber length to produce large forces over a small working range. High power is defined as long fibers and high PCSA therefore muscles capable of producing high forces over a large working range. High shortening velocity is defined as relatively longer fibers with a small PCSA with the muscles produce a small force but contract over a longer distance. Generalized muscles have relatively small force production and fiber lengths

4.1 | Isometry and some muscles of positive allometry in muscle mass throughout the forelimb

The majority of the muscle masses in the Quenda forelimb scaled with isometry, while only one fifth scaled with positive allometry, which suggests that relative muscle size does not change throughout body size growth. Previously published studies have found that generally muscles tend to scale with positive allometry during ontogenetic growth, although findings of isometric scaling are often common (Allen et al., 2010; Lamas et al., 2014; Marchi, Leischner, Pastor, & Hartstone-Rose, 2018; McGowan, Skinner, & Biewener, 2008). Positive allometry of muscles is found in hindlimbs where the interpretation has been than more forceful hindlimb muscles are required for behavior such as escape locomotion (Marchi et al., 2018). Given the strong anatomical patterns consistent with adaptation to digging in the Quenda (Warburton, Grégoire, et al., 2013), we might have expected that more muscles would scale with positive allometry. Consistent with this hypothesis, we found that the six muscles scaled with positive allometry were all muscles that acted as main movers in the power stroke of scratch-digging. Latissimus dorsi (LtD) and serratus ventralis (SeV) were two of the largest proximal placed muscles, and grew with positive allometry. These two muscles would allow the forelimb to retract with a large force against the resistance of the soil, and to stabilize the scapula during the power stroke of digging, respectively.

In the distal forelimb, Quenda have relatively massive carpal and digital flexor muscles. This is consistent with patterns found in other scratch-digging mammals such as the American badger (*Taxidea taxus*), in order to stabilize the carpus during the power stroke of scratch-digging (Moore et al., 2013; Warburton, Grégoire, et al., 2013). In Quenda, the large flexor digitorum profundus (FDP) grew with positive allometry and thus would be able to produce an increasing large force as the animal grows in comparison to the smaller muscles of the forearm that grew with isometry. The FDP is the largest muscles of the forearm, and its increasing relative mass is indicative of its primary role in carpal and digital flexion against the resistance of the soil during digging.

4.2 | Fiber length primarily shows isometry with total body mass

We found that FL primarily scaled with isometry, and of the five muscles in which FL scaled with positive allometry were not confined to either the power-stroke (*n* = 3) or recovery phases (*n* = 2) of scratch-digging. This is consistent with other ontogenetic studies that have found that FL generally scales isometrically within species (Allen et al., 2010). However, as FL is proportional to shortening velocity, longer fibers shorten at greater velocity and therefore are capable of greater power generation, difference in FL between species have been linked to differences in function (Lieber & Ward, 2011; Rose, Nudds, & Codd, 2016). It has been suggested that positive scaling of FL is often associated with muscles for which there is a strong functional signal for particular behavior (i.e., differing diets, different locomotor styles) (Leischner et al., 2018). As such, we might expect that if larger Quenda are digging to a greater extent that FL should have increased with positive allometry. We found that FL of pectoralis (Pec) and

serratus ventralis (SeV) have positive allometry with body mass. These muscles have relatively long fibers generally, and thus the fact that these scale with positive allometry suggests that they become capable of producing relatively greater power as the animal grows. FL also scaled with positive allometry in tensor fascia antebrachii (TFA), pronator quadratus (PrQ), and extensor carpi ulnaris (ECU), suggesting that these muscles rely on FL and therefore shortening velocity for greater power generation.

4.3 | Strong positive allometry in PCSA for majority of forelimb muscles

The majority of muscles had positive allometry of PCSA consistent with other studies (Cuff et al., 2016; Dick & Clemente, 2016; McGowan et al., 2008). This suggests that combinations of factors are involved with the change in muscle force generation as Quenda grow. The 18 muscles that were significantly different from isometry (i.e., scaled with positive allometry) included half the muscles classified as main movers of the power stroke (9/20) and all of the muscles associated with the recovery stroke of scratch-digging (9/9).

As animals grow larger, there are likely to be additional pressures on force production for other behavior including locomotion and the need for balancing large scratch-digging forces with antagonistic forces to help stabilize joints. Positive allometry in PCSA has been found in a range of other studies on ontogenetic scaling of muscles (Allen et al., 2010; Lamas et al., 2014) and is generally interpreted as larger animals requiring relatively greater forces than predicted to support a heavier body mass and muscles involved in locomotion.

It is interesting that all the muscles associated with the recovery stroke showed positive allometry, but not all muscles associated with the power-stroke of scratch-digging did. This significant difference in slope was opposite of our hypothesis that the main movers of the power stroke of scratch-digging would be more likely to grow with positive allometry. While at first, this may appear to suggest differential investment in force production, it could reflect the action of muscles in different regions of the limb. The muscles in the recovery stroke in general are smaller in mass, but may increase their potential force production by modifying their pennation angle in order to increase the number of fibers into a given volume (Zajac, 1992). The carpal and digital flexors and extensors (CDF and CDE) had isometric growth of FL, however generally have a pennation angle of greater than 15°. This allows them to produce a large force from their relatively small muscle mass. In contrast, the main movers of the power stroke have greater capacity to increase potential force production by increasing muscle mass and/or fiber length.

A trade-off between force (PCSA) and speed of contraction (FL) was seen between the smaller forearm muscles (force specialized), and the larger muscles closer to the shoulder that showed relatively longer FL in the Quenda. This trade-off is common, for example, in jaw muscles (Hartstone-Rose, Perry, & Morrow, 2012) and hindlimbs (Marchi et al., 2018) as larger animals have different functional pressures than smaller species. The positive allometry in PCSA of the primate's forelimbs combined with isometry in FL, suggest that larger species rely on stronger forearms while smaller species have relatively faster and more flexible forearms (Leischner et al., 2018). A similar

case was made for interspecific variation in the forelimb muscles of felids (Cuff et al., 2016); however, after a phylogenetic correction was performed, these results were not significant. Our results were consistent with the literature and shows the trade-off which allows relatively smaller muscles to be force specialized.

4.4 | Positive allometry in Fmax for one third of muscles

The isometric hypothesis states that for mechanical similarity, isometric force (N) scales with total body mass to the power of 1.0 (Economos, 1982; Kokshenev, 2008; Rose, 2014). One third (11/29) of Quenda forelimb muscles scaled with positive allometry including half of the power stroke muscles, and one recovery stroke of digging muscles. The remaining two thirds of forelimb muscles in the Quenda are mechanically similar and thus force production remains the same through ontogeny.

In Quenda, we primarily found mechanical similarity across the range of total body sizes. This suggests that smaller body size is not necessarily a disadvantage for smaller animals. In contrast, studies on jackrabbits (*Lepus californicus*), musk-ox (*Ovibos moschatus*), and capuchin monkeys (*Cebus* spp.) have found that juveniles appear to be "over-built" in their musculoskeletal features to compensate for their smaller overall body size (Carrier, 1983; Heinrich, Ruff, & Adamczewski, 1999; Torzilli, Takebe, Burstein, & Heiple, 1981; Young, 2005). These studies were principally related to hindlimbs and thus reflect adaptation for locomotion. Although the isometric force production of small Quenda is absolutely lower than the large individuals, it is unclear to what extent this relates to their digging performance. Data regarding the propensity to dig, the depth of diggings and the substrate selection between small and large individuals might reveal differential behavior that could be associated with muscle development.

4.5 | No sex differences in forelimb muscle mass and architecture

There was negligible difference between males and females in forelimb architecture, although sexual dimorphism is known for this species (Warburton & Travouillon, 2016). Differential muscle growth is reported in species where male–male competition involves fighting with the forelimbs (Martin et al., 2018; Warburton, Bateman, & Fleming, 2013). However, in bandicoot species, male–male fighting involves primarily biting (Johnson, 1989; Stodart, 1966), and is reflected in dimorphism in the dentition for some species, including the Quenda (Flores, Abdala, & Giannini, 2013; Travouillon, Archer, Hand, & Muirhead, 2015; Warburton & Travouillon, 2016). Negligible sexual dimorphism in forelimb musculature in the Quenda is therefore not unexpected.

4.6 | Further considerations

The method of determining if two properties are considered geometrically similar (isometric pattern) or scale with positive or negative allometry has been fairly consistent throughout the literature. The

most commonly used method is using 95% confidence intervals to assess the spread of data points around the regression line, and are classed as isometric if the upper and lower confidence intervals include the relevant value for isometry, that is, mass: 1.0, lengths: 0.33, areas (volumetric property): 0.67 (Allen et al., 2010; Lamas et al., 2014). In comparison, raw values of m_m, FL, and PCSA are transformed by the value of isometry so that predicted regression slopes would be equal to 1.0 (Leischner et al., 2018), or alternatively the raw values are tested against the relevant value of isometry (our study; Cuff et al., 2016). The second less common method requires the calculated slope to be statistically tested against the isometric slope (geometric similarity). Scaling studies will have multiple measures per individual, therefore associated Type 2 errors, which are not controlled when the 95% confidence intervals is the only method of assessing the allometric relationship with the size component (Benjamini & Hochberg, 1995). We suggest using a statistical test to assess the validity of claims of geometric similarity, or positive/negative allometry in addition to using the 95% confidence intervals in further scaling studies.

4.7 | Limitations of this study

Using wild-derived specimens that died of natural causes or as a result of a road accident or dog/cat attack allowed us to collect a large sample size, although there was variation in decomposition and damage to the bodies. Specimens were limited to those in the best condition and steps were taken to reduce these sources of variation. Specimens were frozen as soon as possible to stop decomposition; however, time of death to freezing in some roadkill specimens was longer than euthanized animals. Fixation was required due to the nature of the specimens; to ensure decrease of m_m and FL and allow comparison to fresh-thawed studies, the data was corrected using the correction factors proposed by Kikuchi and Kuraoka (2014). We also note that some animals were from areas where supplementary feeding (i.e., by members of the public) is reported, and as such these animals were potentially overweight (Hillman, Lymbery, Elliot, & Thompson, 2017). Despite these limitations, wild-derived specimens allowed collection of a larger number of individuals that would otherwise have been available, and thus to provide a robust test for intraspecific variation that is often lacking in comparable studies.

5 | CONCLUSIONS

We present the first ontogenetic scaling study of forelimb muscle properties in a scratch-digging mammal. In this marsupial, we found that the force production may be the driving factor in larger individuals benefitting from stronger forelimb muscles, while the smaller individuals rely on relatively faster or more flexible forelimbs for their scratch-digging. The mechanical similarity hypothesis was accepted in two thirds of the forelimb muscles as the maximum isometric force (N) scaled with isometry (slope 1.0). The other third of muscles (half of the main movers of scratch-digging) scaled with positive allometry. This suggests that forelimb muscles force production remains the same through ontogeny for two thirds of the muscles. We have also

made recommendations for methods of scaling assessment for future studies.

Our study emphasizes the importance of intraspecific variation in morphological studies and quantified the ontogenetic muscle architecture. Our results propose questions around the functional behaviors of juveniles in comparison to adults, such as habitat selection and scratch-digging frequencies that can be ultimately tested by behavioral studies.

ACKNOWLEDGMENTS

AUTHOR CONTRIBUTIONS

MLM collected specimens, carried out muscle dissections, measured FL and pennation angles, undertook statistical analysis, and drafted the manuscript, NMW collected specimens, assisted in muscle dissections, produced muscle drawing figures, and drafted the manuscript, KJT drafted the manuscript, and PAF assisted in statistical analysis and drafted the manuscript. All authors contributed to the experimental design and gave final approval for publication. We have no competing interests to declare.

ORCID

Meg L. Martin https://orcid.org/0000-0003-4924-309X
Natalie M. Warburton https://orcid.org/0000-0002-8498-3053
Kenny J. Travouillon https://orcid.org/0000-0003-1734-4742
Patricia A. Fleming https://orcid.org/0000-0002-0626-3851

REFERENCES

Abramoff, M. D., Magalhaes, P. J., & Ram, S. J. (2004). Image processing with ImageJ. *Biophotonics International*, *11*, 7, 36–42.

Allen, V., Elsey, R. M., Jones, N., Wright, J., & Hutchinson, J. R. (2010). Functional specialization and ontogenetic scaling of limb anatomy in *Alligator mississippiensis*. *Journal of Anatomy*, *216*, 423–445. https://doi.org/10.1111/j.1469-7580.2009.01202.x

Allen, V., Molnar, J., Parker, W., Pollard, A., Nolan, G., & Hutchinson, J. R. (2014). Comparative architectural properties of limb muscles in Crocodylidae and Alligatoridae and their relevance to divergent use of asymmetrical gaits in extant Crocodylia. *Journal of Anatomy*, *225*, 569–582. https://doi.org/10.1111/joa.12245

Azizi, E., Brainerd, E. L., & Roberts, T. J. (2008). Variable gearing in pennate muscles. *Proceedings of the National Academy of Sciences of the United States of America*, *105*, 1745–1750. https://doi.org/10.1073/pnas.0709212105

Barnosky, A. D. (1981). A Skeleton of Mesoscalops (Mammalia, Insectivora) from the Miocene deep river formation, Montana, and a review of the Proscalopid moles: Evolutionary, functional, and stratigraphic relationships. *Journal of vertebrate paleontology*, *1*, 285–339. https://doi.org/10.1080/02724634.1981.10011904

Benjamini, Y., & Hochberg, Y. (1995). Controlling the false discovery rate: A practical and powerful approach to multiple testing. *Journal of the Royal Statistical Society. Series B (Methodological)*, *57*, 289–300.

Bennett, M. B., & Garden, J. G. (2004). Locomotion and gaits of the northern brown bandicoot, *Isoodon macrourus*, (Marsupalia: Peramelidae). *Journal of Mammalogy*, *85*, 296–301. https://doi.org/10.2307/1383759

Bertram, J. E. A., & Biewener, A. A. (1990). Differential scaling of the long bones in the terrestrial carnivora and other mammals. *Journal of Morphology*, *204*, 157–169. https://doi.org/10.1002/jmor.1052040205

Böhmer, C., Fabre, A.-C., Herbin, M., Peigné, S., & Herrel, A. (2018). Anatomical basis of differences in locomotor behaviour in martens: A comparison of the forelimb musculature between two sympatric species of *Martes*. *The Anatomical Record*, *301*, 449–472. https://doi.org/10.1002/ar.23742

Carrier, D. R. (1983). Postnatal ontogeny of the musculo-skeletal system in the black-tailed jack rabbit (*Lepus californicus*). *Journal of Zoology*, *201*, 27–55. https://doi.org/10.1111/j.1469-7998.1983.tb04259.x

Channon, A. J., Günther, M. M., Crompton, R. H., & Vereecke, E. E. (2009). Mechanical constraints on the functional morphology of the gibbon hind limb. *Journal of Anatomy*, *215*, 383–400. https://doi.org/10.1111/j.1469-7580.2009.01123.x

Cuff, A. R., Sparkes, E. L., Randau, M., Pierce, S. E., Kitchener, A. C., Goswami, A., & Hutchinson, J. R. (2016). The scaling of postcranial muscles in cats (Felidae) I: Forelimb, cervical, and thoracic muscles. *Journal of Anatomy*, *229*, 128–141. https://doi.org/10.1111/joa.12477

Dick, T. J. M., & Clemente, C. J. (2016). How to build your dragon: Scaling of muscle architecture from the world's smallest to the world's largest monitor lizard. *Frontiers in Zoology*, *13*, 8. https://doi.org/10.1186/s12983-016-0141-5

Economos, A. C. (1982). On the origin of biological similarity. *Journal of Theoretical Biology*, *94*, 25–60. https://doi.org/10.1016/0022-5193(82)90328-9

Fleming, P. A., Anderson, H., Prendergast, A. S., Bretz, M. R., Valentine, L. E., & Hardy, G. E. S. (2014). Is the loss of Australian digging mammals contributing to a deterioration in ecosystem function? *Mammal Review*, *44*, 94–108. https://doi.org/10.1111/mam.12014

Flores, D. A., Abdala, F., & Giannini, N. P. (2013). Post-weaning cranial ontogeny in two bandicoots (Mammalia, Peramelomorphia, Peramelidae) and comparison with carnivorous marsupials. *Zoology*, *116*, 372–384. https://doi.org/10.1016/j.zool.2013.07.003

Gasc, J. P., Jouffroy, F. K., Renous, S., & Blottnitz, F. (1986). Morphofunctional study of the digging system of the Namib Desert golden mole (*Eremitalpa granti namibensis*): cinefluorographical and anatomical analysis. *Journal of Zoology*, *208*, 9–35. http://doi.org/10.1111/j.1469-7998.1986.tb04706.x

Gordon, G., & Hulbert, A. J. (1989). Peramelidae. In D. W. Walton & B. J. Richardson (Eds.), *Fauna of Australia. Mammalia* (Vol. 1B, pp. 603–624). Canberra: Australian Government Publishing Service.

Hammer, Ø., Harper, D. A. T., & Ryan, P. D. (2001). PAST: Paleontological statistics software package for education and data analysis. *Palaeontologia Electronica*, *41*, 9. http://palaeo-electronica.org/2001_1/past/issue1_01.htm

Hartstone-Rose, A., Perry, J. M. G., & Morrow, C. J. (2012). Bite force estimation and the fiber architecture of felid masticatory muscles. *The Anatomical Record*, *295*, 1336–1351.

Heinrich, R. E., Ruff, C. B., & Adamczewski, J. Z. (1999). Ontogenetic changes in mineralization and bone geometry in the femur of musk-oxen (*Ovibos moschatus*). *Journal of Zoology*, *247*, 215–223.

Hildebrand, M. (1977). Analysis of asymmetrical gaits. *Journal of Mammalogy*, *58*, 131–156. https://doi.org/10.2307/1379571

Hildebrand, M. (1985). Digging of quadrupeds. In M. Hildebrand, D. M. Bramble, K. F. Liem, & B. D. Wake (Eds.), *Functional vertebrate morphology* (pp. 89–109). Cambridge, MA: The Blknap Press of Harvard Univeristy Press.

Hillman, A. E., Lymbery, A. J., Elliot, A. D., & Thompson, R. C. A. (2017). Urban environments alter parasite fauna, weight and reproductive activity in the quenda (*Isoodon obesulus*). *Science of the Total Environment*, *607*, 1466–1478.

Hopkins, S. S. B. & Davis, E. B. (2009). Quantitative morphological proxies for fossoriality in small mammals. *Journal of Mammalogy*, *90*, 1449–1460. http://doi.org/10.1644/08-mamm-a-262r1.1

Johnson, C. N. (1989). Social interactions and reproductive tactics in red–necked wallabies (*Macropus rufogriseus banksianus*). *Journal of Zoology*, *217*, 267–280. https://doi.org/10.1111/j.1469-7998.1989.tb02487.x

Kikuchi, Y. (2010). Comparative analysis of muscle architecture in primate arm and forearm. *Anatomia, Histologia, Embryologia*, *39*, 93–106. https://doi.org/10.1111/j.1439-0264.2009.00986.x

Kikuchi, Y., & Kuraoka, A. (2014). Differences in muscle dimensional parameters between non-formalin-fixed (freeze-thawed) and formalin-fixed specimen in gorilla (*Gorilla gorilla*). *Mammal Study*, *39*, 65–72. https://doi.org/10.3106/041.039.0101

Kokshenev, V. B. (2008). A force-similarity model of the activated muscle is able to predict primary locomotor functions. *Journal of Biomechanics*, *41*, 912–915. https://doi.org/10.1016/j.jbiomech.2007.11.005

Lagaria, A., & Youlatos, D. (2006). Anatomical correlates to scratch digging in the forelimb of European ground squirrels (*Spermophilus citellus*). *Journal of Mammalogy*, *87*, 563–570. https://doi.org/10.2307/4094514

Lamas, L. P., Main, R. P., & Hutchinson, J. R. (2014). Ontogenetic scaling patterns and functional anatomy of the pelvic limb musculature in emus (*Dromaius novaehollandiae*). *PeerJ*, *2*, e716. https://doi.org/10.7717/peerj.716

Leischner, C. L., Crouch, M., Allen, K. L., Marchi, D., Pastor, F., & Hartstone-Rose, A. (2018). Scaling of primate forearm muscle architecture as it relates to locomotion and posture. *The Anatomical Record*, *301*, 484–495. https://doi.org/10.1002/ar.23747

Lessa, E. P., & Thaeler, C. S. (1989). A reassessment of morphological specializations for digging in pocket gophers. *Journal of Mammalogy*, *70*, 689–700. http://doi.org/10.2307/1381704

Lieber, R. L., & Fridén, J. (2000). Functional and clinical significance of skeletal muscle architecture. *Muscle & Nerve*, *23*, 1647–1666. https://doi.org/10.1002/1097-4598(200011)23:11<1647:AID-MUS1>3.0.CO;2-M

Lieber, R. L., & Ward, S. R. (2011). Skeletal muscle design to meet functional demands. *Philosophical Transactions of the Royal Society B: Biological Sciences*, *366*, 1466–1476. https://doi.org/10.1098/rstb.2010.0316

McIntosh, A. F., & Cox, P. G. (2016a). Functional implications of craniomandibular morphology in African mole-rats (Rodentia: Bathyergidae). *Biological Journal of the Linnean Society*, *117*, 447–462. http://doi.org/10.1111/bij.12691

McIntosh, A. F., & Cox, P. G. (2016b). The impact of gape on the performance of the skull in chisel-tooth digging and scratch digging mole-rats (Rodentia: Bathyergidae). *Royal Society Open Science*, *3*, 160568. http://doi.org10.1098/rsos.160568

Marchi, D., Leischner, C. L., Pastor, F., & Hartstone-Rose, A. (2018). Leg muscle architecture in primates and its correlation with locomotion patterns. *The Anatomical Record*, *301*, 515–527. doi:10.1002/ar.23745

Martin, M. L., Bateman, P. W., Auckland, C. H., Miller, D. W., Warburton, N. M., Barnes, A. L., & Fleming, P. A. (2018). Is there evidence for a trade-off between sperm competition traits and forelimb musculature in the western grey kangaroo? *Biological Journal of the Linnean Society*, *123*, 431–444. https://doi.org/10.1093/biolinnean/blx151

McGowan, C. P., Skinner, J., & Biewener, A. A. (2008). Hind limb scaling of kangaroos and wallabies (superfamily Macropodoidea): Implications for hopping performance, safety factor and elastic savings. *Journal of Anatomy*, *212*, 153–163. https://doi.org/10.1111/j.1469-7580.2007.00841.x

Medler, S. (2002). Comparative trends in shortening velocity and force production in skeletal muscles. *American Journal of Physiology-Regulatory, Integrative and Comparative Physiology*, *283*, 368–378. https://doi.org/10.1152/ajpregu.00689.2001

Mendez, J., & Keys, A. (1960). Density and composition of mammalian muscle. *Metabolism*, *9*, 184–188.

Michilsens, F., Vereecke, E. E., D'Août, K., & Aerts, P. (2009). Functional anatomy of the gibbon forelimb: Adaptations to a brachiating lifestyle. *Journal of Anatomy*, *215*, 335–354. https://doi.org/10.1111/j.1469-7580.2009.01109.x

Moore, A. L., Budny, J. E., Russell, A. P., & Butcher, M. T. (2013). Architectural specialization of the intrinsic thoracic limb musculature of the American badger (*Taxidea taxus*). *Journal of Morphology*, *274*, 35–48. https://doi.org/10.1002/jmor.20074

Myatt, J. P., Crompton, R. H., Payne-Davis, R. C., Vereecke, E. E., Isler, K., Savage, R., … Thorpe, S. K. S. (2012). Functional adaptations in the forelimb muscles of non-human great apes. *Journal of Anatomy*, *220*, 13–28. https://doi.org/10.1111/j.1469-7580.2011.01443.x

Olson, R. A., Womble, M. D., Thomas, D. R., Glenn, Z. D., & Butcher, M. T. (2015). Functional morphology of the forelimb of the nine-banded armadillo (*Dasypus novemcinctus*): Comparative perspectives on the myology of Dasypodidae. *Journal of Mammalian Evolution*, *23*, 1–21. https://doi.org/10.1007/s10914-015-9299-4

Picasso, M. B. J. (2015). Ontogenetic scaling of the hindlimb muscles of the greater Rhea (*Rhea americana*). *Anatomia, Histologia, Embryologia*, *44*, 452–459. https://doi.org/10.1111/ahe.12158

Quinn, G. P., & Keough, M. J. (2002). *Experimental design and data analysis for biologists*. Cambridge, UK: Cambridge University Press.

Rose, J., Moore, A., Russell, A., & Butcher, M. (2014). Functional osteology of the forelimb digging apparatus of badgers. *Journal of Mammalogy*, *95*, 543–558. https://doi.org/10.1644/13-mamm-a-174

Rose, J. A. (2014). *Hindlimb morphology in eastern cottontail rabbits (Sylvilagus floridanus): Correlation of muscle architecture and MHC isoform content with ontogeny* (Master of Science in Biology Masters). Youngstown State University, Ohio. Retrieved from http://rave.ohiolink.edu/etdc/view?acc_num=ysu1403279058

Rose, J. A., Sandefur, M., Huskey, S., Demler, J. L., & Butcher, M. T. (2013). Muscle architecture and out-force potential of the thoracic limb in the eastern mole (*Scalopus aquaticus*). *Journal of Morphology*, *274*, 1277–1287. https://doi.org/10.1002/jmor.20178

Rose, K. A., Nudds, R. L., & Codd, J. R. (2016). Variety, sex and ontogenetic differences in the pelvic limb muscle architectural properties of leghorn chickens (*Gallus Gallus domesticus*) and their links with locomotor performance. *Journal of Anatomy*, *228*, 952–964. https://doi.org/10.1111/joa.12460

Rupert, J. E., Rose, J. A., Organ, J. M., & Butcher, M. T. (2015). Forelimb muscle architecture and myosin isoform composition in the groundhog (*Marmota monax*). *The Journal of Experimental Biology*, *218*, 194–205. https://doi.org/10.1242/jeb.107128

Shimer, H. W. (1903). Adaptations to aquatic, arboreal, fFossorial and cursorial habits in mammals. III. Fossorial adaptations. *The American Naturalist*, *37*, 819–825. https://doi.org/10.2307/2455381

Stein, B. R. (2000). Morphology of subterranean rodents. In A. Lacey, J. L. Patton, & G. N. Cameron (Eds.), *Life underground: the biology of subterranean rodents* (pp. 19–61). Chicago: The Univeristy of Chicago Press.

Stodart, E. (1966). Management and behaviour of breeding groups of the marsupial *Perameles nasuta* Geoffroy in captivity. *Australian Journal of Zoology*, *14*, 611–623. https://doi.org/10.1071/ZO9660611

Thorpe, S. K. S., Crompton, R. H., GÜnther, M. M., Ker, R. F., & McNeill, A. R. (1999). Dimensions and moment arms of the hind- and forelimb muscles of common chimpanzees (*Pan troglodytes*). *American Journal of Physical Anthropology*, *110*, 179–199. https://doi.org/10.1002/(SICI)1096-8644(199910)110:2<179:AID-AJPA5>3.0.CO;2-Z

Torzilli, P. A., Takebe, K., Burstein, A. H., & Heiple, K. G. (1981). Structural properties of immature canine bone. *Journal of Biomechanical Engineering*, *103*, 232–238. https://doi.org/10.1115/1.3138286

Travouillon, K. J., Archer, M., Hand, S. J., & Muirhead, J. (2015). Sexually dimorphic bandicoots (Marsupialia: Peramelemorphia) from the Oligo-Miocene of Australia, first cranial ontogeny for fossil bandicoots and new species descriptions. *Journal of Mammalian Evolution*, *22*, 141–167. https://doi.org/10.1007/s10914-014-9271-8

Travouillon, K. J., & Phillips, M. J. (2018). Total evidence analysis of the phylogenetic relationships of bandicoots and bilbies (Marsupialia: Peramelemorphia): Reassessment of two species and description of a new species. *Zootaxa*, *4378*, 224–256. doi:10.11646/zootaxa.4378.2.3

Valentine, L. E., Anderson, H., Hardy, G. E. S., & Fleming, P. A. (2013). Foraging activity by the southern brown bandicoot (*Isoodon obesulus*) as a mechanism for soil turnover. *Australian Journal of Zoology*, *60*, 419–423. https://doi.org/10.1071/ZO13030

Vassallo, A. I. (1998). Functional morphology, comparative behaviour, and adaptation in two sympatric subterranean rodents genus *Ctenomys* (Caviomorpha: Octodontidae). *Journal of Zoology*, *244*, 415–427. http://doi.org/10.1111/j.1469-7998.1998.tb00046.x

Warburton, N. M., Bateman, P. W., & Fleming, P. A. (2013). Sexual selection on forelimb muscles of western grey kangaroos (Skippy was clearly a female). *Biological Journal of the Linnean Society*, *109*, 923–931. https://doi.org/10.1111/bij.12090

Warburton, N. M., Grégoire, L., Jacques, S., & Flandrin, C. (2013). Adaptations for digging in the forelimb muscle anatomy of the southern brown bandicoot (*Isoodon obesulus*) and bilby (*Macrotis lagotis*). *Australian Journal of Zoology*, *61*, 402–419. https://doi.org/10.1071/ZO13086

Warburton, N. M., & Travouillon, K. J. (2016). The biology and palaeontology of the Peramelemorphia: a review of current knowledge and future research directions. *Australian Journal of Zoology*, *64*, 151–182. https://doi.org/10.1071/ZO16003

Williams, S. B., Wilson, A. M., Rhodes, L., Andrews, J., & Payne, R. C. (2008). Functional anatomy and muscle moment arms of the pelvic limb of an elite sprinting athlete: The racing greyhound (*Canis familiaris*). *Journal of Anatomy*, *213*, 361–372. https://doi.org/10.1111/j.1469-7580.2008.00961.x

Young, J. W. (2005). Ontogeny of muscle mechanical advantage in capuchin monkeys (*Cebus albifrons* and *Cebus apella*). *Journal of Zoology*, *267*, 351–362. https://doi.org/10.1017/S0952836905007521

Zajac, F. E. (1992). How musculotendon architecture and joint geometry affect the capacity of muscles to move and exert force on objects: A review with application to arm and forearm tendon transfer design. *The Journal of hand surgery*, *17*, 799–804. https://doi.org/10.1016/0363-5023(92)90445-U

SUPPORTING INFORMATION

Additional supporting information may be found online in the Supporting Information section at the end of the article.